

TRANSVERSE GRADIENT UNDULATORS FOR A STORAGE RING X-RAY FEL OSCILLATOR*

R.R. Lindberg[†] and K.-J. Kim, ANL Advanced Photon Source, Argonne, IL 60439, USA,
Y. Cai, Y. Ding, and Z. Huang, SLAC National Accelerator Laboratory, Menlo Park, CA 94025, USA

Abstract

An x-ray FEL oscillator (XFEL) is a fully coherent 4th generation source with complementary scientific applications to those based on self-amplified spontaneous emission. While the naturally high repetition rate, intrinsic stability, and very small emittance produced by an ultimate storage ring (USR) makes it a potential candidate to drive an XFEL, the energy spread is typically an order of magnitude too large for sufficient gain. On the other hand, Smith and coworkers showed how the energy spread requirement can be effectively mitigated with a transverse gradient undulator (TGU): since the TGU has a field strength that varies with transverse position, by properly correlating the electron energy with transverse position one can approximately satisfy the FEL resonance condition for all electrons. Motivated by the recent work in the high-gain regime we investigate the utility of a TGU for low gain FELs at x-ray wavelengths. We find that a TGU may make an XFEL realizable in the largest ultimate storage rings now under consideration (e.g., in either the old Tevatron or PEP-II tunnel).

INTRODUCTION

Storage rings have served the synchrotron radiation community with bright x-rays from spontaneous emission for over fifty years. Additionally, some have produced coherent, intense radiation in the infrared to ultraviolet spectral range using free-electron laser (FEL) oscillators. Hence, it is natural to consider whether the storage rings of today might also drive an FEL oscillator operating at x-ray wavelengths. As shown in Ref. [1], such an x-ray FEL oscillator (XFEL) is feasible with current linac-based e-beams using a stabilized Bragg crystal-based x-ray optical cavity. Unfortunately, the equilibrium electron beam brightness of modern third generation storage rings is not sufficient for the XFEL: both the transverse emittance and the energy spread is too large to provide sufficient FEL gain. With the recent advances in minimum emittance lattices, however, so-called “ultimate storage rings” are being designed that can satisfy the transverse emittance condition $\varepsilon_x \sim \varepsilon_y \lesssim \lambda/4\pi$ at hard x-ray wavelengths. On the other hand, the longitudinal brightness in a storage ring is still too poor: the equilibrium energy spread is more than an order of magnitude too large, with a typical value

$$\sigma_\gamma/\gamma \equiv \sigma_\eta \sim 0.1\%.$$

To make the large energy spread of a storage ring beam compatible with FEL operation, Smith and collaborators [2] proposed designing the undulator field such that the dimensionless deflection parameter $K \equiv eB_0/mck_u$ varies transversely as shown in Fig. 1 (here B_0 is the peak magnetic field, $k_u \equiv 2\pi/\lambda_u$ is the undulator wave-vector, and e, m, c are the electron charge magnitude, mass, and speed of light). Then, by combining this transverse gradient undulator (TGU) field with an electron beam whose energy is also correlated with transverse position, one can imagine preserving FEL gain even in the presence of large energy spreads. The TGU concept was recently revisited for high-gain FELs driven by large energy spread beams produced by laser-plasma accelerators in Ref. [3], and for high-gain FELs in a USR by Ref. [4].

In this paper we investigate to what extent one might leverage the advances in ultimate storage ring design with a TGU to drive an x-ray free-electron laser oscillator (XFEL). First, we begin by reviewing some basic low-gain TGU physics, and show that the parameter regime for XFELs is somewhat different than that used in Refs. [5, 6]. Hence, we reinterpret some of their results, and then use some relatively simple analytic expressions to describe the TGU effect as it pertains to x-ray parameters. These expressions can be derived from the more complete 3D gain analysis that we sketch in the Appendix. Next, we discuss how the ideas developed for the TGU-FEL can be applied at x-ray wavelengths, and show how XFEL operation may become viable in a TGU with an electron beam whose energy spread is of order 0.1%, provided the emittance is $\lesssim \lambda/4\pi$. Finally, we begin to explore what additional constraints are imposed if this e-beam is derived from a stable, high brightness, ultimate storage ring (USR). It appears to be quite difficult to operate the XFEL in a USR without some sort of bypass line, and we further find that maintaining sufficient peak current and realistic kicker times are quite challenging. Nevertheless, we show that there are a set of parameters for which a storage ring TGU-XFEL is compatible with the PEP-X ring design [7].

FEL PHYSICS WITH A TGU

FEL gain requires a resonant interaction between the electrons and the radiation field. Writing the fundamental radiation wavelength as $\lambda_1 \equiv 2\pi/k_1$, the FEL interaction requires that

$$\lambda_1 = \lambda_u \frac{1 + K^2/2}{2\gamma^2} \quad (1)$$

* Work supported by U.S. Dept. of Energy, Office of Science, Office of Basic Energy Sciences, under Contract No. DE-AC02-06CH11357

[†] lindberg@aps.anl.gov

be approximately satisfied for almost all of the particles in the beam, where γ is the electron's Lorentz factor. For this reason, traditional FELs require e-beams with very small energy spreads: for a low gain device the FEL bandwidth scales $\sim 1/N_u$ and we require $\sigma_\eta \ll 1/N_u$. Ref. [2] showed that this constraint can be relaxed by designing the undulator field to vary transversely and then sorting the incoming electrons such that those with higher energy see a stronger field than those with lower energy such that the resonance condition (1) is satisfied for all electrons.

For example, the decreasing undulator gap in Fig. 1 results in a B -field that is an increasing function of x , meaning that one would ideally position the electrons so that their energy is a monotonically increasing function of x . Specifically, we want

$$\lambda = \lambda_u \frac{1 + K^2(x_j)/2}{2\gamma_j^2} \equiv \lambda_u \frac{1 + K^2(x_j)/2}{2\gamma_0^2(1 + \eta_j)^2} \quad (2)$$

for each electron indexed by j , where $\eta_j \equiv (\gamma_j - \gamma_0)/\gamma_0$ is the normalized energy deviation from the reference energy γ_0 . We approximately satisfy Eq. (2) for all electrons by introducing dispersion upstream of the undulator that correlates the electron's energy and position according to

$$x_j = D\eta_j + x_{\beta_j}, \quad (3)$$

where D is the dispersion strength and x_{β_j} is the residual position whose initial value equals the transverse coordinate before the dispersion section. Assuming a linear dependence of K near the origin, $K(x) \approx K_0(1 + \alpha x)$ with α the transverse magnetic field gradient, we insert the coordinate (3) into the resonance condition (2) to find

$$\begin{aligned} \lambda &= \lambda_u \frac{1 + K^2(D\eta_j + x_{\beta_j})/2}{2\gamma_0^2(1 + \eta_j)^2} \\ &\approx \lambda_u \frac{1 + K_0^2/2}{2\gamma_0^2} \left[1 + \frac{K_0^2\alpha(D\eta_j + x_{\beta_j})}{1 + K_0^2/2} - 2\eta_j \right]. \end{aligned} \quad (4)$$

Now, we can eliminate η_j from the resonance condition (4) and effectively remove the influence of energy spread by choosing

$$\alpha D = \frac{2 + K_0^2}{K_0^2}. \quad (5)$$

Note that this TGU cancellation is only important if the beam size in the undulator is dominated by the dispersion, namely, if the beam size before the dispersive section $\langle x_{\beta_j}^2 \rangle \equiv \sigma_x^2 \ll D^2\sigma_\eta^2$.

Further analysis of the TGU-FEL was performed by Kroll, Rosenbluth, and collaborators [5, 6], who found that FEL emission/gain in a TGU also excites transverse betatron oscillations, and that using a TGU to increase the acceptable energy spread by a factor of R implied that the required emittance was reduced by a factor $1/R$. These results apply in the limit that the electron beam executes many betatron oscillations in the natural focusing provided by the transverse gradient, which is typically far from satisfied at x-ray wavelengths. In fact, to lowest order we

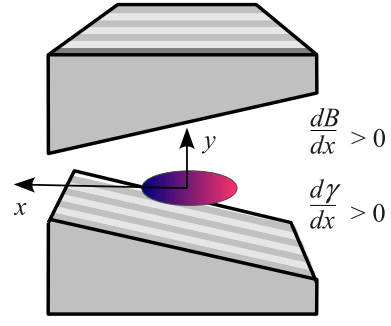


Figure 1: Schematic of a transverse gradient undulator, where the field gradient is due to the variation in the magnetic gap obtained by canting the undulator poles. If the e-beam energy is correlated in x according (5) then the requirement on the energy spread can be greatly reduced.

can typically ignore the natural undulator focusing for the high energy e-beams required for x-ray FELs, while the gradient-induced focusing strength is a factor $\alpha/k_u \ll 1$ smaller; hence, we will discuss a different TGU limit relevant to XFEL operation.

FEL Gain in a TGU

We can acquire some basic understanding of the FEL gain in a TGU by considering a one-dimensional (1D) model for an e-beam with a Gaussian energy spread σ_η . The 1D gain G for an undulator of $N_u \equiv L_u/\lambda_u$ periods and a beam of peak current I is

$$\begin{aligned} G &= -\frac{2\pi^2}{\gamma} \frac{I}{I_A} \frac{K_0^2[\text{JJ}]^2}{1 + K_0^2/2} \frac{N_u^3 \lambda_1^2}{2\pi \Sigma_x \Sigma_y} \\ &\times \int_{-1/2}^{1/2} ds dz \sin[2\pi N_u \Delta\nu(z-s)] \\ &\times (z-s) e^{-2[2\pi N_u(z-s)\sigma_\eta]^2}. \end{aligned} \quad (6)$$

Here, $\Delta\nu \equiv \nu - 1 \equiv (\omega - \omega_1)/\omega_1$ is the frequency difference from FEL resonance, $I_A \equiv 4\pi\epsilon_0 mc^3/e \approx 17$ kA is the Alfvén current with ϵ_0 the permittivity of free space, the Bessel function factor $[\text{JJ}] \equiv J_0[K_0^2/(4 + 2K_0^2)] - J_1[K_0^2/(4 + 2K_0^2)]$, and $\Sigma_{x,y}^2 \equiv \sigma_{x,y}^2 + \sigma_{r_{x,y}}^2$ are the convolved transverse sizes in terms of the rms e-beam ($\sigma_{x,y}$) and radiation ($\sigma_{r_{x,y}}$) sizes. The gain expression (6) reproduces the well-known formula for a low-gain FEL when $\sigma_\eta \rightarrow 0$, and it can be easily related to the standard convolution of the mono-energetic gain with the energy spread (see, e.g., [8]), or derived from the fully 3D analysis of Ref. [9] and the Appendix.

We simplify the gain equation (6) by assuming that the Rayleigh range is of order $L_u/2\pi$ and that the electron and radiation beam sizes are matched to maximize their overlap,

$$\Sigma_x = \Sigma_y \approx \sqrt{2}\sigma_r = \sqrt{\frac{\lambda_1 Z_R}{2\pi}} \approx \frac{\sqrt{\lambda_1 L_u}}{2\pi}, \quad (7)$$

so that the gain becomes

$$G = -\frac{4\pi^3}{\gamma} \frac{I}{I_A} \frac{K_0^2 [\text{JJ}]^2}{1 + K_0^2/2} \frac{N_u^2 \lambda_1}{\lambda_u} \times \int_{-1/2}^{1/2} ds dz \sin[2\pi N_u \Delta\nu(z-s)] \times (z-s) e^{-2[2\pi N_u(z-s)\sigma_\eta]^2}. \quad (8)$$

If the energy spread can be neglected, meaning that $(2\pi\sigma_\eta)^2 \ll 1/N_u^2$, then the integral gives the usual derivative of the sinc²($2\pi N_u \Delta\nu$) associated with spontaneous emission. This factor depends only on $N_u \Delta\nu$, so that the gain increases as N_u^2 when $\sigma_\eta \rightarrow 0$. In the opposite limit when the energy spread dominates, the integrand is negligible unless $|z-s| \lesssim 1/N_u \sigma_\eta$ and $\Delta\nu \approx \sigma_\eta$, so that the integral scales $\sim 1/N_u^2 \sigma_\eta^2$ and G is independent of the number of undulator periods. Upon maximizing G with respect to $\Delta\nu$ an accurate fitting formula that describes the 1D gain for arbitrary energy spreads is

$$G_{\text{FEL}} \approx \frac{4\pi^3}{\gamma} \frac{I}{I_A} \frac{K_0^2 [\text{JJ}]^2}{1 + K_0^2/2} \frac{\lambda_1}{\lambda_u} \frac{0.27 N_u^2}{1 + (5.46 N_u \sigma_\eta)^2} \equiv g_0 \frac{N_u^2}{1 + (5.46 N_u \sigma_\eta)^2}, \quad (9)$$

where we have introduced the constant g_0 that is independent of N_u and σ_η .

On the other hand, from Eq. (4) we see that the resonance spread for a TGU-enabled FEL is given by x_{β_j}/D rather than η_j , while the beam size along x is dominated by the dispersion. Hence, we can understand the TGU's gain properties by making the replacements $\sigma_\eta \rightarrow \sigma_x/D$ and $\Sigma_x \rightarrow (\sigma_x^2 + \sigma_{r,x}^2 + D^2 \sigma_\eta^2)^{1/2} \approx D\sigma_\eta$ in (6); using a similar analysis we find that the TGU gain formula analogous to Eq. (9) is

$$G_{\text{TGU}} \approx g_0 \frac{\sqrt{2} N_u^2 / \sigma_\eta}{D/\sigma_x + (5.46 N_u)^2 \sigma_x / D}. \quad (10)$$

This expression can also be derived from the 1D limit of Eq. (27) in the Appendix, for which $\mathcal{D}_x = \mathcal{D}_y = 1$ and $\Sigma_\phi \rightarrow 0$. For large energy spreads ($N_u^2 \sigma_\eta^2 \gg 1$) the ratio of the TGU gain to that of a standard FEL is given by

$$\frac{G_{\text{TGU}}}{G_{\text{FEL}}} \approx \frac{D\sigma_\eta}{\sigma_x} \frac{\sqrt{2}}{1 + [D/(5.46 N_u \sigma_x)]^2}. \quad (11)$$

We see that the gain of the TGU first increases with increasing dispersion D as the larger x - γ correlation mitigates the variation of the FEL resonance condition. Once the energy spread effect is effectively cancelled, however, increasing the dispersion and e-beam size further leads to a decrease in the FEL coupling and, hence, G . Equation (10) predicts that the TGU gain is maximized when $D/\sigma_x = 5.46 N_u$, in which case we immediately find that a TGU can increase the gain in a long undulator by a factor of

$$\frac{G_{\text{TGU}}}{G_{\text{FEL}}} \approx 5.46 N_u \sigma_\eta = \frac{D\sigma_\eta}{\sigma_x} \gg 1. \quad (12)$$

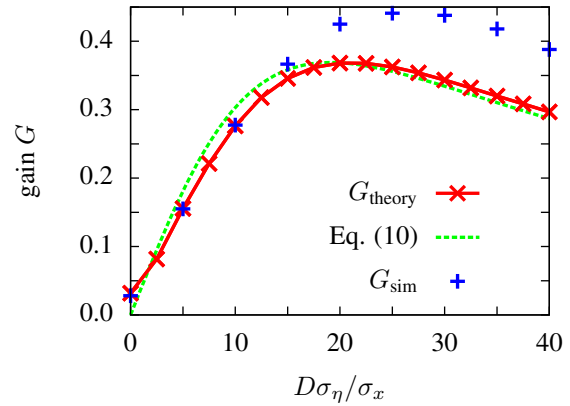


Figure 2: Gain as a function of the expansion parameter $D\sigma_\eta/\sigma_x$ using the parameters of Table 1. In solid red is the maximized gain using the theory of the Appendix, while the green dotted line plots the simple 1D-type prediction of Eq. (10) scaled to match the maximum of G_{theory} . In blue we plot simulation results using the parameters from the maximization of G_{theory} .

Essentially, the gain can be increased in proportion to the amount that the e-beam size is expanded due to the induced dispersion upstream of the FEL. This result applies for long undulators such that $N_u \gg 1/\sigma_\eta$ when the effects of emittance and diffraction are small ($\varepsilon_{x,y} \lesssim \lambda_1/4\pi$).

We plot the anticipated FEL gain as a function of $D\sigma_\eta/\sigma_x$ in Fig. 2. Here we have used the basic e-beam and undulator parameters from Table 1, although we vary D , α , and the e-beam and radiation optics to maximize G at each point. The red solid theory line graphs the predictions based on the theory of the Appendix [i.e., Eq. (27)], which has been maximized with respect to the frequency difference $\Delta\nu$, the x -Rayleigh range in Z_{R_x} , and the y -beta-function at the waist $\beta_y^* = \sigma_y/\varepsilon_y$ assuming that $Z_{R_y} = \beta_y^* = \sigma_x^2/\varepsilon_x$; the full theory is closely followed by the simple 1D-type prediction of Eq. (10), which we scale to match the maximum of G_{theory} . Finally, we plot in blue the 3D, time-independent simulation results for the gain. All results predict that a TGU can increase G by more than an order of magnitude over the standard $\alpha = D = 0$ FEL that has $G \approx 3\%$. The gain curve from full numerical simulations is similar to that of our theory, although G_{sim} is about 10% bigger at large dispersions D . While this level of accuracy is to be expected since the next order correction to the theory scales $\sim (G-1)^2 \sim 10\%$, we do not understand why the discrepancy is asymmetric.

A TGU-enabled X-ray FEL Oscillator

We have discussed how a TGU may enable FEL operation for beams with large energy spreads, used relatively simple arguments to show that the increase in gain scales roughly as (12), and provided an explicit formula (27) for

Table 1: Sample Parameters for a TGU-enabled XFEL Operating at a Photon Energy of 14.4 keV

e-Beam		Undulator	
I	20 A	N_u	2500
σ_z/c	2 ps	λ_u	1.63 cm
$\gamma_0 m c^2$	6 GeV	L_u	40.75 m
σ_η	0.14 %	K_0	1.0
$\varepsilon_x = \varepsilon_y$	5.2 pm	α	34 /m
D	8.8 cm	ave gap	7 mm
β_y^*	7.3 m		
Radiation		FEL output	
λ_1	0.886 Å	$P(G = 0.2)$	19 MW
Z_{R_x}	105 m	Est. $\Delta\omega/\omega_1$	$< 10^{-7}$
Z_{R_y}	7.3 m	Est. P_{out}	~ 1 MW
linear G	0.44	Est. $N_{\text{ph out}}$	$\sim 10^9$

the gain in a TGU including the effects of the applied dispersion, the e-beam energy spread and emittance, and radiation diffraction when the natural undulator focusing can be neglected. In this section we will show results for the TGU gain using parameters that anticipate those of the potential PEP-X ultimate storage ring [7].

We list representative e-beam, undulator, radiation, and FEL parameters for a TGU-enabled XFEL designed to generate 14.4 keV photons in Table 1. The energy, emittance, and energy spread are typical of the very large ultimate storage rings that are presently being considered, but the longitudinal e-beam width σ_z and hence, the peak current, is somewhat unique to the PEP-X design [7]. The latter I is considerably larger than, for example, that of the proposed Tevatron-based USR [10]. Since the linear FEL gain is directly proportional to I this is an important point, and we will return to discuss it more fully in the next section.

The undulator parameters are quite similar to those first proposed in [1], with the main differences being that the XFEL in Table 1 is designed for 14.4 keV photons and the magnetic field gap along the axis (labelled ‘‘ave gap’’) has been increased to 7 mm. The undulator gradient satisfies the TGU condition (5), with the dispersion D in Table 1 designed for a TGU expansion of $D\sigma_\eta/\sigma_x \approx 20$. We can estimate the required variation in the magnetic field gap to produce this α by repeating the arguments of [3] that are based on the Halbach formula for the on-axis field of a Samarium-Cobalt permanent magnetic device:

$$B_0[T] \propto \exp\left[-\frac{g}{\lambda_u} \left(5.47 - 1.8 \frac{g}{\lambda_u}\right)\right]$$

$$\Rightarrow \alpha \equiv \frac{1}{B_0} \frac{dB_0}{dx} \approx \frac{3.6g - 4.47\lambda}{\lambda^2} \frac{dg}{dx}. \quad (13)$$

Hence, for the gap $g = 7$ mm and period $\lambda_u = 1.63$ cm we estimate that each pole will have to be angled by ~ 0.07 radians with respect to the horizontal.

Using these nominal e-beam and undulator parameters, we plot in 3(a) the theoretical FEL gain as a function of the

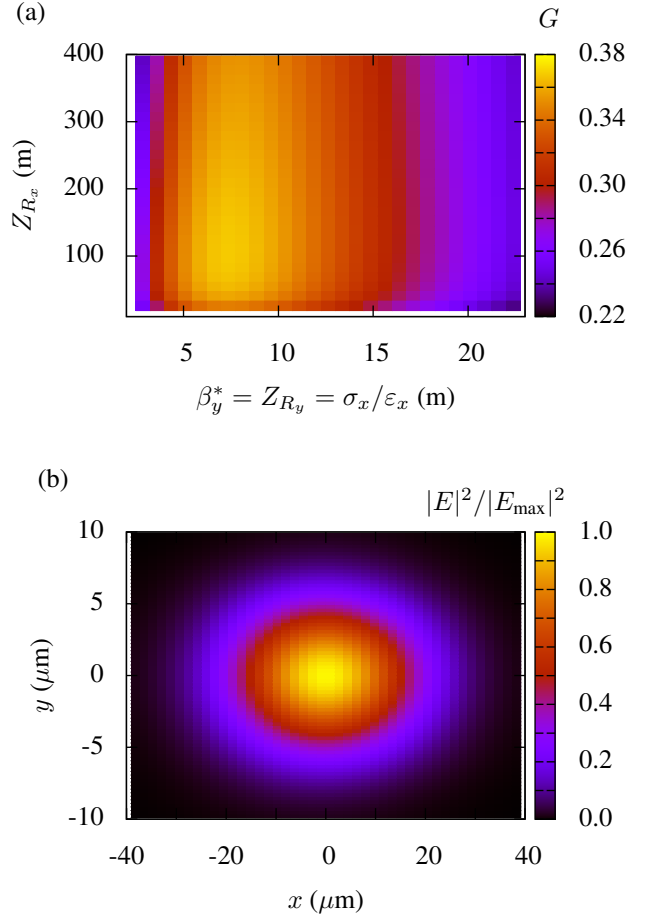


Figure 3: (a) Theoretically predicted gain as a function of $\beta_y = Z_{R_y} = \sigma_x^2/\varepsilon_x$ at the undulator center and the x -Rayleigh range Z_{R_x} for the parameters of Table 1. (b) Simulated profile of the FEL mode at its waist as imaged by 1 : 1 optics. We used $Z_{R_y} = 7.3$ m and $Z_{R_x} = 105$ m, while the aspect ratio of the radiation (e-beam) is measured to be approximately 3.7 : 1 (20 : 1).

e-beam β_y -function at the waist and the radiation x -Rayleigh range Z_{R_x} . Here, we use the theory of the Appendix with the e-beam focusing such that $\beta_y(L_u/2) = \sigma_x^2/\varepsilon_x = Z_{R_y}$, which we have found to yield approximately the maximum of G . Note that while this theory somewhat underestimates the actual gain as shown in Fig. 2, FEL simulations verify that the functional dependence of G on the e-beam and radiation focusing parameters are quite similar to that shown here. For example, the gain depends very weakly on the Rayleigh range Z_{R_x} , decreasing by only a few percent as one quadruples Z_{R_x} from about 100 to 400 m. This may allow one to eliminate one of the focusing mirrors along x (this is not possible in y since $Z_{R_y} \lesssim 10$ m).

In Fig. 3(b) we show the simulated image of the mode shape at the undulator center when the e-beam β -functions and radiation Rayleigh ranges are chosen to maximize the

gain (exact parameters are listed in Table 1). Here, the mode that maximizes the gain is elliptical, although not as elongated as the electron beam – while the aspect ratio of the e-beam is about 20 : 1, it is only about 3.7 : 1 for the mode of maximum gain. As mentioned earlier we can further increase Z_{R_x} without significantly changing the gain, which would yield a more asymmetric mode. Regardless, since the field is coherent this asymmetry can be removed with appropriate focusing or with the reflection from an asymmetric Bragg crystal; for the initial input here that is Gaussian ($M_x M_y = 1$), the field after FEL amplification was measured to have $M_x M_y < 1.01$.

Finally, we list the anticipated XFEL field properties in the column FEL output of Table 1. For example, we find that the nonlinear effects of particle trapping reduce the gain to 20% when the cavity power is about 20 MW, so that if the total cavity losses are 20% and we couple 5% of the field out of the cavity than the estimated output power is about 1 MW. Since we do not yet have a time-dependent FEL simulation for the entire TGU-based XFEL, at this point we only estimate the normalized bandwidth and photon number by scaling previous results for a standard XFEL. Based on these results, we predict that the normalized bandwidth can be as low as 2×10^{-8} , while we expect that the total number of coherent photons to be a few $\times 10^9$; thus, we believe that the numbers listed in Table 1 are conservative. For this number of coherent photons the source brightness is between 10^{33} and 10^{34} photons/[mm²mrad²s(0.1% BW)].

AN ULTIMATE STORAGE RING-BASED XFEL

Synchrotron light sources based on electron storage rings have grown tremendously around the world over the past two decades. Today these 3rd generation light sources use high energy, low emittance electron beams and undulator insertion devices to produce high brightness x-rays. Typical e-beam energies range from 1.5 to 8 GeV, while the natural emittance of the stored beam is typically between 1 to 10 nm-rad as determined by the beam energies, the magnet lattice properties, and the ring circumference. Advances in lattice design have opened the door to USRs whose emittances are in the picometer regime. We discuss some additional constraints required if the ring to drive XFEL, and then discuss how the PEP-X design is particularly well-suited for doing this.

USR Constraints from XFEL Requirements

Experience has shown that an FEL oscillator does not produce stable output when it is operated as a normal insertion device in a storage ring. Rather, the FEL and the ring act as coupled oscillators in which long time-scale (compared to the time between bunches) oscillations in FEL power are out of phase with oscillations in e-beam energy spread and emittance [11]. Since the operation of a TGU-

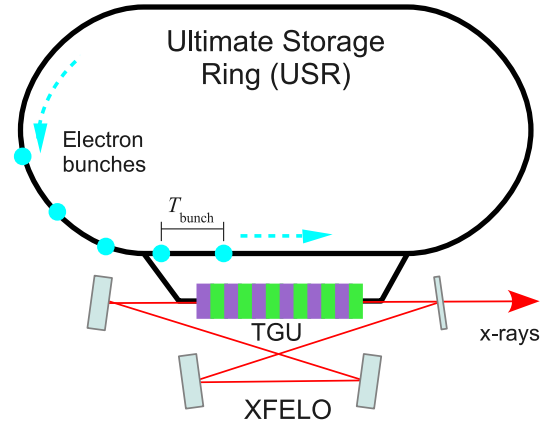


Figure 4: Schematic of an x-ray FEL oscillator in a bypass line of an ultimate storage ring.

based XFEL is fine-tuned to the assumed partitioning of the electron beam phase space, it appears to be best to decouple the storage ring beam dynamics with that of the XFEL by operating a pulsed FEL in a bypass of the USR as illustrated in Fig. 4.

For an XFEL in a bypass, a sequence of electron bunches whose temporal spacing matches the round trip time of the optical pulse in the x-ray cavity T_{cavity} is selected from the storage ring and directed into the bypass line by means of a fast pulsed kicker magnet. The bunches drive the XFEL to saturation, with each “used” bunch being returned to the ring so that the increased energy spread/emittance can be damped back to their equilibrium values. If the storage ring damping times $\tau_{x,y,z}$ are longer than the time required for the XFEL to use every stored electron bunch, then the XFEL must be turned off for the remaining time.

We assume that the $N_{\text{bunch}} \gg 1$ stored electron bunches in the ring are temporally spaced from one another by $T_{\text{bunch}} = C_{\text{ring}}/cN_{\text{bunch}}$ as shown in Fig. 4, where C_{ring} is the ring circumference. Hence, to operate the bypass line we require a fast kicker magnet with rise and fall time $T_{\text{kicker}} < T_{\text{bunch}}$ to direct one electron bunch into the bypass at a time. Successive bunches in the XFEL bypass are temporally spaced by T_{cavity} , meaning that the kicker fires at a repetition rate equal to $1/T_{\text{cavity}}$. Thus, the kicker rise/fall time T_{kicker} , its period of operation T_{cavity} , and the electron bunch spacing in the ring T_{bunch} are related by

$$T_{\text{kicker}} < T_{\text{bunch}} \leq T_{\text{cavity}}. \quad (14)$$

Equation (14) describes the important role played by the full width duration of the kicker: T_{kicker} puts a lower bound on the spacing between the electron bunches, which in turn leads to an upper bound on the number of stored bunches $N_{\text{bunch}} = C_{\text{ring}}/cT_{\text{bunch}}$. N_{bunch} is critical for determining how long the XFEL can operate before the FEL interaction degrades the energy spread and emittance of the stored beam. For a large USR with a sufficient number of

stored bunches such that the storage ring damping times $\tau_{x,y,z} \ll N_{\text{bunch}} T_{\text{cavity}}$, than the beam returns to its high-brightness equilibrium before being kicked back into the bypass, so that the XFEL can be constantly operated. On the other hand, if the $\tau_{x,y,z}$ are too long than the FEL interaction can degrade the beam energy spread and emittance after each bunch is used approximately once. In this case the XFEL must be turned off after producing x-rays over a time $\sim N_{\text{bunch}} T_{\text{cavity}}$, and only returned to operation once the ring approaches its equilibrium after 3-4 damping times.

Fast kickers are currently being developed in a number of laboratories around the world. One of the most promising devices that may be adapted to a USR is the International Linear Collider prototype developed at KEK-ATF, which has been demonstrated in tests to have $T_{\text{kicker}} \lesssim 5$ ns [12]. Hence, in what follows we will only consider rings whose bunch spacing $T_{\text{bunch}} \sim 5$ -10 ns, which in turn typically limits the XFEL to a pulsed mode of operation so that the e-beam may be returned to its high-brightness equilibrium; further improvements in fast kickers may permit an XFEL to be run all the time.

The timing relations (14) constrain the bunch pattern in the storage ring, while requiring the gain to be $\gtrsim 30\%$ puts strong limits on the emittance and peak bunch current. For the largest USRs the emittance $\varepsilon_x \sim \varepsilon_y \lesssim \lambda_1/4\pi$ at angstrom wavelengths, in which case achieving sufficient peak I is the primary concern.

PEP-X Design

Most third generation storage rings have lattices that are built with repetitive cells known as double-bend or triple-bend achromats. To further reduce the emittance in a storage ring one must pack more magnets within a cell or increase its circumference to accommodate more cells.

Recently, a 7-bend achromat lattice was proposed in Sweden for the MAX-IV project [13], achieving a natural emittance of 0.25 nm-rad at 3 GeV in a 500-meter storage ring. This remarkable breakthrough was possible largely because of a technology of building compact magnets developed in the MAX-lab in many years. Simply scaling the MAX-IV ring from 0.5 to 2.2 km in circumference while retaining its cell structure, one could have a storage ring with 12 pm-rad emittance at 6-GeV beam energy.

This simple USR design philosophy was adopted by Ref. [7] and then extended using an improved method to optimize the dynamic aperture to propose a potential USR to be situated in the the old positron-electron project (PEP) ring. This PEP-X storage ring design reduces the natural emittance by converting the straight sections of PEP into arcs to form a circular machine. Additionally, the proposal uses the superconducting RF cavities developed for the CEBAF upgrade project [14] to longitudinally shorten the electron bunch. By applying an 80-MV accelerating gradient at a frequency of 1.5 GHz, the bunch length could be made as short as 2 ps, thereby increasing the peak cur-

Table 2: Main Parameters of the PEP-X Ultimate Storage Ring

Parameter	Description	Value
C_{ring}	circumference	2234.21 m
$\gamma_0 m c^2$	beam energy	6.0 GeV
$\varepsilon_{x,y}$	x,y emittances	5.2, 5.2 pm-rad
σ_η	energy spread	1.39×10^{-3}
σ_z	bunch length	0.60 mm
$\tau_{x,y,z}$	damping times	13, 15, 9 ms

rent of a 100 pC bunch to about 20 A. The main parameters of the lattice are tabulated in Table 2.

As we have shown in Table 1 and Fig. 3, these USR parameters are sufficient to produce single pass FEL gains $\sim 40\%$ for 14.4 keV photons. On the other hand, we still must determine a bunch pattern that satisfies (14) and has enough stored electron bunches to have a significant amount of steady state XFEL operation. Previous studies have shown that XFELs similar to that described in Table 1 typically requires ~ 500 passes to reach a steady state where the fluctuations are $\lesssim 1\%$; hence, we would like the ring to store $N_{\text{bunch}} \gtrsim 1000$ bunches to have enough steady state x-ray pulses for the users, while the total number of available accelerating buckets is 11170.

We imagine filling every 10th bucket, which implies that we store 1117 bunches spaced every $T_{\text{bunch}} = C_{\text{ring}}/cN_{\text{bunch}} \approx 6.67$ ns, which is larger than the measured 5 ns kicker rise/fall time for KEK-ATF prototype. As shown in Fig. 3, the gain is maximized when $Z_R \approx 7.5$ m, which implies that a reasonable distance between the mirrors for optical stability is 75-100 m with a round trip optical path length twice that. This distance is reasonably well matched to the 186 m path length required if we kick out every 93rd bunch, so that $T_{\text{cavity}} \approx 0.647$ μ s. In addition, the timing pattern so described uses every electron bunch exactly once in the FEL before repeating.

Every electron bunch has contributed to the FEL gain and suffered significant reductions in 6D brightness after approximately 0.72 ms. At this time the XFEL must be turned off for at least $3\tau_y \sim 45$ ms to return to its equilibrium, meaning that the XFEL duty factor will be between 1% and 2%. Even when operating 1% of the time, an XFEL producing x-rays with the single pulse characteristics of Table 1 at repetition rate of ≈ 1.5 MHz will have a time averaged brightness $\approx 10^{26}$ photons/[mm²mrad²s(0.1% BW)].

In principle one might able to operate the XFEL constantly by filling every bucket and increasing the cavity length by about a factor of 5-8. This, however, would require confronting two significant technological challenges: the longer x-ray optical cavity would have more stringent stabilization conditions, and the kicker rise/fall times would have to be reduced below one nanosecond.

Other Potential USR-based XFELs

It appears that there is a rather limited parameter space for a TGU-enabled XFEL operating at an ultimate storage ring. Nevertheless, we have shown that it may be possible to operate such a device at the PEP-X USR. Similar sized rings should also be able to accommodate the required bunch pattern/spacing for the XFEL bypass. On the other hand, it may not be as trivial to reproduce the comparatively high ($\gtrsim 10$ A) peak current. The PEP-X design benefits from a naturally small momentum compaction and also employs strong rf to focus the bunch longitudinally, both of which contribute to a short electron bunch that is still below the microwave instability threshold. We have found that other ultimate storage rings presently being considered have insufficient peak currents for FEL gain.

For example, the nominal design of the very large 9 GeV USR proposed for the old Tevatron initially appeared to be quite attractive from an FEL standpoint. However, the nominal bunch length becomes considerably longer once nonlinear and collective effects are included [10], and the peak current of about 4 A leads to an FEL gain of only 10%. We have found one way to improve the FEL gain is by changing the emittance partition/coupling in the storage ring: while the design in [10] has unit coupling ($\varepsilon_x = \varepsilon_y$), one might significantly reduce the emittance in the vertical plane by decreasing the coupling. In this case the nominal beam size σ_y can also be decreased. If one then orients the TGU-FEL such that the gap is vertical (i.e., rotates Fig. 1 by 90°) and disperses the beam along y than the gain can be improved significantly. The increase in G is primarily due to the smaller beam size in the dispersed direction for a given TGU gain enhancement $\sim D\sigma_\eta/\sigma_y$, while the output field profile can be round. On the other hand, decreasing the coupling leads to an increase in ε_x due to intrabeam scattering, which may not be ideal for operations. Nevertheless, preliminary indications are that G can be increased to 30% in the Tevatron-based USR even with the low peak currents, while gains twice that shown in Table 1 are possible at PEP-X.

CONCLUSIONS

We have shown that a transverse gradient undulator can enable useful FEL gains $\gtrsim 30\%$ at hard x-ray wavelengths for electron beams with $\sigma_\gamma/\gamma_0 \approx 0.1\%$ provided that $\varepsilon_{x,y} \lesssim \lambda/4\pi$ and $I \gtrsim 10$ A. These beam parameters are close to those of the largest ultimate storage rings presently under consideration, and it may be possible to use a future USR to drive a TGU-enabled x-ray FEL oscillator in a bypass line. While the USR is strongly constrained by the relatively large peak currents and short kicker rise/fall times preferred by XFEL operation, we have shown a set of parameters for which an XFEL is possible within the PEP-X USR design. Such a (pulsed) device would produce hard x-rays of unparalleled spectral flux and stability to vastly improve the reach of many scientific experiments.

APPENDIX: 3D THEORY OF FEL GAIN

The linearized transverse electron equations of motion including the effects of the TGU are

$$\frac{dx}{dz} = p_x \quad \frac{dp_x}{dz} = -\frac{K^2\alpha^2}{2\gamma_0}x \equiv -k_x^2x \quad (15)$$

$$\frac{dy}{dz} = p_y \quad \frac{dp_y}{dz} = -\frac{K^2(k_u^2 + \alpha^2)}{2\gamma_0}x \equiv -k_y^2y, \quad (16)$$

which differ from the standard equations by the additional focusing provided by the undulator gradient α . In the above we have assumed that a uniform, static magnetic field of strength $(mc/e)(K^2\alpha/2\gamma_0)$ has been added to cancel the net bending that results from the asymmetric wiggle motion due to the transverse gradient. The longitudinal equations are

$$\frac{d\theta_j}{dz} = 2k_u\eta_j - k_u \frac{K_0^2\alpha x_j}{1 + K_0^2/2} - \frac{k_1}{2} (p_j^2 + k_x^2 x_j^2) \quad (17)$$

$$\frac{d\eta_j}{dz} = \frac{eK[\text{JJ}]}{2\gamma_0^2 mc^2} \int d\nu d\phi E_\nu(\phi; z) e^{i\nu\theta_j} e^{ik_1\phi \cdot \mathbf{x}_j} + c.c., \quad (18)$$

where $E_\nu(\phi; z)$ is the electric field amplitude in the frequency-angular representation, whose coordinates are the normalized frequency ν and the transverse angle from the axis $\phi = (\phi_x, \phi_y)$. Note that the energy spread effect in the phase equation (17) cancels if $\eta_j = K_0^2\alpha x_j/(2 + K_0^2)$, reproducing condition (5).

The FEL amplification in the low-gain limit can be found using the method proposed in Ref. [9], in which the linearized equations for the electron distribution function and the field are solved assuming that the change in E_ν is small. We introduce the distribution F_ν describing the microbunching near the fundamental frequency $\nu \approx 1$, whose linearized Boltzmann equation is given by

$$\frac{\partial F_\nu}{\partial z} + i\nu \frac{d\theta}{dz} F_\nu + \frac{d\mathbf{x}}{dz} \cdot \frac{\partial F_\nu}{\partial \mathbf{x}} + \frac{d\mathbf{p}}{dz} \cdot \frac{\partial F_\nu}{\partial \mathbf{p}} = -\frac{d\eta}{dz} \frac{\partial \bar{F}}{\partial \eta}, \quad (19)$$

where \bar{F} is the smooth, background distribution around $\nu \approx 0$ that we assume is in some sense much bigger than F_ν . Hence, the equation governing the background distribution is approximately independent of F_ν , and \bar{F} evolves along the unperturbed trajectories associated with (15)-(16).

In terms of F_ν , the Maxwell equation is

$$\left(\frac{\partial}{\partial z} + ik_u \Delta\nu + \frac{ik_1}{2} \phi^2 \right) E_\nu(\phi; z) = -\frac{en_e K[\text{JJ}]}{2\lambda_1^2 \epsilon_0 \gamma_0} \int d\eta d\mathbf{x} d\mathbf{p} e^{-ik_1\phi \cdot \mathbf{x}} F_\nu(\eta, \mathbf{x}, \mathbf{p}; z), \quad (20)$$

where n_e is the electron density. As mentioned previously, the low-gain solution to (19)-(20) was derived for a standard undulator ($\alpha = 0$) in Ref. [9], and a particularly elegant expression for the gain was determined when the transverse focusing can be neglected; specifically, it was

shown that the gain can be written as a convolution over the brightness fields of the input radiation, the undulator radiation, and the electron beam distribution \bar{F} . A structurally similar result for the gain can be found from the equations above.

Rather than write out the long calculation whose details closely follow [9], we will merely sketch the steps involved. We first solve the Boltzmann equation (19) by integrating along the unperturbed trajectories (characteristics), which when inserted into (20) leads to an integral equation for the electric field. In the low-gain limit a closed form solution for E_ν can be obtained using the first term in the Liouville-Neumann series solution (i.e., the Born approximation). In the limit of negligible focusing relevant to XFELs, $1 \gg k_y L_u \gg k_x L_u$, the gain can be written as

$$G = \frac{n_e (eK[\text{JJ}])^2}{4\lambda_1^2 \epsilon_0 \gamma_0^3 m c^2} \int d\eta d\mathbf{p} d\phi d\mathbf{x} d\mathbf{q} \mathcal{B}_E(\mathbf{q}, \phi + \mathbf{p}) \times \frac{\mathcal{B}_U(\eta, \mathbf{x}, \phi, \alpha q_x, \alpha p_x) \frac{\partial}{\partial \eta} \bar{F}(\eta, \mathbf{x} + \mathbf{q}, \mathbf{p})}{\int d\psi d\mathbf{y} \mathcal{B}_E(\mathbf{y}, \psi)}, \quad (21)$$

where the radiation brightness

$$\mathcal{B}_E(\mathbf{x}, \phi) \equiv \int d\xi e^{-ik_1 \mathbf{x} \cdot \boldsymbol{\xi}} E_\nu^*(\phi + \frac{\boldsymbol{\xi}}{2}) E_\nu(\phi - \frac{\boldsymbol{\xi}}{2}), \quad (22)$$

while the undulator ‘‘brightness’’

$$\mathcal{B}_U \equiv \int_{-L_u/2}^{L_u/2} dz ds \int d\xi e^{i(\Delta\nu - \eta)k_u(z-s)} e^{-ik_1 \mathbf{x} \cdot \boldsymbol{\xi}} \times e^{ik_1(\phi + \boldsymbol{\xi}/2)^2 z/2} e^{-ik_1(\phi - \boldsymbol{\xi}/2)^2 s/2} \times e^{\frac{iK_0 \alpha}{1 + K_0^2/2} [x + q_x + p_x(z+s)/2] k_u(z-s)}; \quad (23)$$

note that \mathcal{B}_U in (23) is the standard undulator brightness when $\alpha \rightarrow 0$, in which case the last line above becomes unity and the gain formula (21) simplifies to a convolution over brightness functions.

We can simplify the abstract gain formula (21) to a semi-analytic expression that we have found to be quite useful when trying to quickly optimize G by assuming a Gaussian distribution for both the input field E_ν and the background electron distribution function:

$$\mathcal{B}_E(\mathbf{x}, \phi) = \exp\left(-\frac{x^2}{2\sigma_{r_x}^2} - \frac{y^2}{2\sigma_{r_y}^2}\right) \times \exp\left(-\frac{\phi_x^2}{2\sigma_{\phi_x}^2} - \frac{\phi_y^2}{2\sigma_{\phi_y}^2}\right) \quad (24)$$

$$\bar{F}(\eta, \mathbf{x}, \mathbf{p}) = \frac{e^{-\eta^2/2\sigma_\eta^2}}{(2\pi)^{3/2} \epsilon_x \sigma_\eta} \exp\left(-\frac{x^2}{2\sigma_x^2} - \frac{y^2}{2\sigma_y^2}\right) \times \frac{1}{2\pi \epsilon_y} \exp\left(-\frac{p_x^2}{2\sigma_{p_x}^2} - \frac{p_y^2}{2\sigma_{p_y}^2}\right). \quad (25)$$

Using the brightness fields (24)-(25) and the undulator definition (23) in the expression of G results in an unruly expression that can be tamed with a number of careful Gaussian integrations; all but two integrals can be done

analytically. We obtain even simpler final expressions by assuming that the gradient and dispersion are related by

$$\alpha D = \frac{2 + K_0^2}{K_0^2} \frac{D^2 \sigma_\eta^2}{D^2 \sigma_\eta^2 + \sigma_x^2}. \quad (26)$$

The condition (26) agrees with (5) when $\sigma_x^2 \ll D^2 \sigma_\eta^2$ and the TGU is effective, while having a straightforward limit for vanishing α and/or D . Then, the TGU-FEL gain becomes

$$G = -\frac{2\pi^2}{\gamma} \frac{I}{I_A} \frac{K_0^2 [\text{JJ}]^2}{1 + K_0^2/2} \frac{N_u^3 \lambda_1^2}{2\pi \Sigma_x \Sigma_y} \times \int_{-1/2}^{1/2} dz ds \exp\left\{-\frac{2[2\pi N_u(z-s)\sigma_\eta \sigma_x]^2}{\sigma_x^2 + D^2 \sigma_\eta^2}\right\} \times \frac{(z-s) \exp[2\pi i N_u \Delta\nu(z-s)]}{i\sqrt{\mathcal{D}_x \mathcal{D}_y}} \times \exp\left\{-\frac{[2\pi N_u L_u(z-s)^2 D \sigma_{p_x} \sigma_\eta]^2}{2(\sigma_x^2 + D^2 \sigma_\eta^2)^2}\right\}, \quad (27)$$

where we have defined the transverse factors $\mathcal{D}_{x,y}$ in terms of the convolved sizes and divergences

$$\Sigma_x \equiv \sqrt{\sigma_x^2 + \sigma_{r_x}^2 + D^2 \sigma_\eta^2} \quad \Sigma_{\phi_x} \equiv \sqrt{\sigma_{p_x}^2 + \sigma_{\phi_x}^2} \quad (28)$$

$$\Sigma_y \equiv \sqrt{\sigma_y^2 + \sigma_{r_y}^2} \quad \Sigma_{\phi_y} \equiv \sqrt{\sigma_{p_y}^2 + \sigma_{\phi_y}^2} \quad (29)$$

via

$$\mathcal{D}_{x,y} \equiv 1 + z s \frac{L_u^2 \Sigma_{\phi_{x,y}}^2}{\Sigma_{x,y}^2} - i \left[(z-s) k_1 L_u \Sigma_{\phi_{x,y}}^2 + \frac{(z-s)L_u}{4k_1 \Sigma_{x,y}^2} \right]. \quad (30)$$

Note that in the 1D limit $\mathcal{D}_{x,y} = 1$ and $\Sigma_{\phi_{x,y}} = 0$, so that the expression above has an identical form to (6).

The general gain formula derived above shows that the energy spread effect is characterized by the dimensionless parameter $2\pi N_u \sigma_x / \sqrt{D^2 + \sigma_x^2 / \sigma_\eta^2}$ when the dispersion and undulator gradient are related by (26); G has the appropriate limits for large and vanishing dispersion, and at the waist the convolved beam size in x has contributions from the natural e-beam and radiation widths along with the beam size increase due to dispersion. The factor on the last line of (27) limits the gain when the x -divergence disrupts the x - γ correlation required for TGU energy spread compensation; this effect is small provided $(\sigma_p N_u L_u / D)^2 \sim [(\sigma_p / \sigma_x) L_u]^2 \ll 1$, which is typically the case.

ACKNOWLEDGMENT

We acknowledge Michael Borland for useful discussions on ultimate storage rings and Marc Ross for informing us on kicker performance.

REFERENCES

- [1] K.-J. Kim, Y. Shvyd'ko and S. Reiche, Phys. Rev. Lett. **100** (2008) 244802.
- [2] T.I. Smith, L.R. Elias, J.M.J. Madey, and D.A.G. Deacon, J. Appl. Phys. **50** (1979) 4580.
- [3] Z. Huang, Y. Ding, and C.B. Schroeder, Phys. Rev. Lett. **109** (2012) 204801.
- [4] Y. Ding, P. Baxevanis, Y. Cai, Z. Huang, and R. Ruth, IPAC'13, Shanghai, China, May 2013, WEPWA075.
- [5] N.M. Kroll, P.L. Morton, M.N. Rosenbluth, J.N. Eckstein, and J.M.J. Madey, IEEE J. Quantum Electron. **17** (1981) 1496.
- [6] N.M. Kroll and M.N. Rosenbluth, J. de Physique **44** (1983) C1-85.
- [7] Y. Cai, K. Bane, R. Hettel, Y. Nosochkov, M.-H. Wang, and M. Borland, Phys. Rev. ST-AB **15** (2012) 054002.
- [8] G. Dattoli, P.L. Ottaviani, A. Segreto, and G. Altobelli, J. Appl. Phys. **15** (1995) 6162.
- [9] K.-J. Kim, Nucl. Instrum. Methods Phys. Res. A **318** (1992) 489.
- [10] M. Borland, IPAC'12, New Orleans, May 2012, TUPPP033, p. 1683, <http://www.JACoW.org>.
- [11] P. Elleaume, J. de Physique **45** (1984) 997.
- [12] T. Naito, S. Araki, H. Hayano, K. Kubo, S. Kuroda, N. Terunuma, T. Okugi, and J. Urakawa, Phys. Rev. ST Accel. Beams **14** (2011) 051002.
- [13] S.C. Leemann, Å. Andersson, M. Eriksson, L.-J. Lindgren, E. Wallén, J. Bengtsson, and A. Streun, Phys. Rev. ST Accel. Beams **12**, 120701 (2011).
- [14] J. Benesch et al., Proceedings of 2005 Particle Accelerator Conference, Knoxville, Tennessee, 1482 (2005).